2020 IEEE/RSJ International Conference on Intelligent Robots and Systems (IROS)
October 25-29, 2020, Las Vegas, NV, USA (Virtual)

A Horse Inspired Eight-wheel Unmanned Ground Vehicle with Four-swing Arms

Miaolei HE
College of Engineering and Design
Hunan Normal University
Changsha, China
rchml@hotmail.com

Jilin He, Changji Ren, Qinghua He
College of Mechanical and Electrical Engineering
Central South University
Changsha, China

***Abstract*—Rigid-terrain unmanned ground vehicles(UGV) can run under the field environment by the advanced adaptive ability. This paper presents a novel horse inspired rigid-terrain eight-wheel vehicle with four-swing arms. This unmanned ground vehicle is drived by distributed hydraulic motors. By cooperating with four-swing arms and eight wheels, the vehicle has the ability to work like a horse climbs an obstacle under the complex ground. The mechanism, bionic obstacle surmounting algorithm and operation strategy are analyzed in detail. The posture planning of wheel arms and the kinematic model of the UGV are studied. Automatic Dynamic Analysis of Mechanical Systems (ADAMS) simulation results and prototype experiments are executed to verify the analysis and strategy. The results show that this type of unmanned ground vehicle has good performance on crossing the obstacle and running on the rigid-terrain ground.**

***Index Terms*—unmanned ground vehicle; obstacle surmount; dynamic analysis**

I. INTRODUCTION

The UGV is a kind of special platform without drives, can execute many tasks in the hostile environment [1]–[3].Cause the strong ability of environmental adaptation and intelligence by equipping many different sensors, the UGV has been widely applied in both civil and military operations [4], [5]. Following the definition in [6], UGVs can be classified as wheeled type, tracked type, legged type and composite style. During these types, the wheel-legged composite one has aroused much attention from many researchers [7]–[10] , for its fast moving speed, climbing ability and environment adaption.

The UGV is always working in the unstructured environment. So it is the basic requirement for the UGV to has good adaptation and obstacle-surmounting ability. Many types of wheel-legged UGV are proposed. Kim *et al.* proposed a wheel-transformer UGV [11] with passive-transform wheels, which are segmented into three independent legs, can climb an 3.25 times wheel-radius height obstacle. A transform-wheel-leg UGV, based on the crank slider mechanism principle, was proposed by Sun *et al.* [12]. It had leg and wheel modes, which helped the vehicle cross an obstacle wither the height of 2.67 times the wheel radius. All these UGVs use the transform mechanism to realize obstacles surmounting, which will affect the mobility of the UGV. So researchers studied the redundant mechanism type vehicle to improve the performance of the UGV. A shrimp inspired robot with parallel suspension architectures was proposed by Sigwart *et al.* in [13], it could cross an obstacle with the height of 2.67 times the wheel radius. These works proved that using the redundant mechanism can improve performance to a certain degree.To get a good stability performance for the negative-mechanism robot, Grand *et al.* developed a wheel-legged UGV using posture control algorithm in [14] . The robot was equipped with four articulated legs to balance the platform when crossing an obstacle. The bogie structure is an efficient design for the UGV. An articulated vehicle with multiple bogies and axles was proposed in [15], the special structure of the vehicle helped the platform have excellent ground-contact ability when moving on the ground.

However, all these UGVs mentioned above do not have sufficient reliability and load capacity, which limits the application in the real word. A ”Guardium” vehicle [15] with double-wishbone suspensions has the advantages of strong maneuverability and 35% self weight payload, but the obstacle climbing ability is limited. The ”Crusher” UGV [16] was developed to meet heavy-payload requirement. It could bear load about near 60% self weight and negotiate a 2.4 times wheel-radius height wall, by using a six-swing-arms structure.

This paper proposes a novel wheel-legged UGV, named as ”Dragon Horse”. The obstacle surmounting strategy is inspired by horse clearing the fence, as shown in Fig. 1. The platform has four-swing horse-like arms, which makes the UGV surmount a vertical obstacle easily by planning the arms posture. Equipped with the hydraulic drive system, the Horse Dragon has sufficient power to supply for the surmounting scenario, also has excellent payload ability. This paper is organized as follows. In section II,the structure model of the UGV is introduced. In section III the obstacle surmounting strategy is studied in detail.In section IV some simulation and experimental results are given to verify the efficiency of the Dragon Horse.

Fig. 1. the Horse Clears a Fence

II. Structure of the Dragon Horse

A. Horse Inspired Concept

The structure design of the Dragon Horse is inspired by the horse clearing a fence, as show in Fig. 1. The horse can adjust its legs posture to cross it. Meanwhile, by controlling the legs action, the horse can balance its gravity center and surmount the fence at high speed. Inspired by this motion mechanism, we design four swing arms for the Dragon Horse, as show in Fig. 2(a). And the structure of the swing arm is shown in Fig. 2(b).

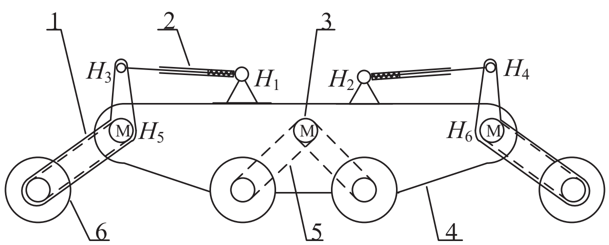

(a)Structure Diagram of the Vehicle Body:1.Swing-arm 2.Hydraulic cylinder 3.Motor 4.Chassis 5.Transmission chain 6.Tire

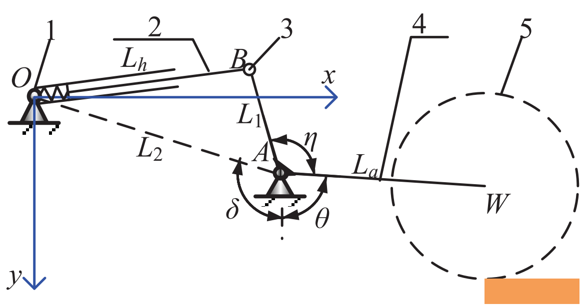

(b)The arm geometry model:1. hip joint 2. thigh 3. knee joint 4. swing arm 5. wheel

Fig. 2. Structure of the Dragon Horse

The chassis of Dragon Horse is equipped with a set of swing arms, which can swing around the hinge point $H_{5,6}$, drived by the six wheel-side hydraulic motors. The transmission system is the chain-gear driving type. As shown in Fig. 2, point O is the hip joint, which connects the chassis and the swing-arm; point B is the knee joint; and A is fixed to the Dragon Horse body. OB is the hydraulic cylinder, and BAW is the swing-arm. The hydraulic cylinder can change the stroke to drive the thigh to elongate or retract. During the operating process, the swing arms can rotate around A. The degree of freedom (DOF) can be expressed as:

$$M = d(n - g - 1) + \sum_{i=1}^{g} f_i - \zeta \tag{1}$$

where n is the connection number;g is the joints number; f_i is the DOF at i joint; and ζ is the local-DOF number. For this type of structure, $d = 3$. Follow this method, we can obtain the DOF of swing arm, $M = 2$. When the four swing arms are controlled by a planning law, Dragon Horse platform can contact with the ground during the vehicle surmounting the obstacle.

Based on the geometry model, the relationship between hydraulic cylinder stroke L_h and the swing angle θ can be expressed as:

$$L_h = \sqrt{L_1^2 + L_2^2 - 2L_1L_2\cos(\delta + \eta + \theta)} \tag{2}$$

where δ and η are shown in Fig. 2(b). And the coordinate system is build as in the Fig. 2(b). The function of the wheel center coordinate can be obtained:

$$\begin{cases} x_W = L_a \sin\theta + L_2 \sin\delta \\ y_W = L_a \cos\theta - L_2 \cos\delta \end{cases} \tag{3}$$

Based on the parameters of the platform in TABLE 1, the values are set as: $L_a$is the arm length, $L_a = 705mm$, $L_1 = 420mm$, $L_2 = 1400mm$, $\delta = 108°$, $\eta = 115°$, and $\theta = \begin{bmatrix} 30° & 110° \end{bmatrix}$.

B. Kinematic model of the UGV

The transform swing arms of the Dragon Horse are used to surmount obstacles. So it is reasonable for us to build a kinematic model for the wheel center and the hydraulic cylinder displacement. It is not only a theory basis for the UGV design, but also a guide to the platform strategy design. By analyzing the movement mechanism, the relationship between the wheel center velocity and the arm angular rate can be obtained:

$$\begin{cases} \dot{s} = J(\theta) \cdot \dot{\theta} \\ s = \begin{bmatrix} x & y \end{bmatrix}^T \end{cases} \tag{4}$$

where $J(\theta)$ is the Jacobian matrix of the swing arm. Combined with Eq.4, we can obtain:

$$J(\theta) = L_a[\cos\theta \quad -\sin\theta]^T \tag{5}$$

The swing-arm angular rate can be expressed as:

$$\dot{\theta} = J\left(L_h\right)\dot{L}_h \tag{6}$$

where the $J(L_h)$ is the Jacobian matrix of the hydraulic cylinder. Substitute the Eq.2 into Eq.6, we can obtain:

$$J\left(l_h\right) = \frac{L_h}{L_1L_2}\left[1 - \left(\frac{L_1^2 + L_2^2 - L_h^2}{2L_1L_2}\right)^2\right]^{-\frac{1}{2}} \tag{7}$$

Combine Eq.4-7, the kinematic model of swing arms can be obtained as:

$$\begin{cases} x = \int \frac{L_a L_h}{L_1 L_2}\left[1-\left(\frac{L_1^2+L_2^2-L_h^2}{2L_1L_2}\right)^2\right]^{-\frac{1}{2}} \cos\theta dL_h \\ y = -\int \frac{L_a L_h}{L_1 L_2}\left[1-\left(\frac{L_1^2+L_2^2-L_h^2}{2L_1L_2}\right)^2\right]^{-\frac{1}{2}} \sin\theta dL_h \end{cases} \tag{8}$$

C. the Dragon Horse platform

The control system of Dragon Horse is composed of a remote controller, a ground-station computer, an onboard vehicle computer, a hydraulic driving system and a swing arms system, as show in Fig. 3.

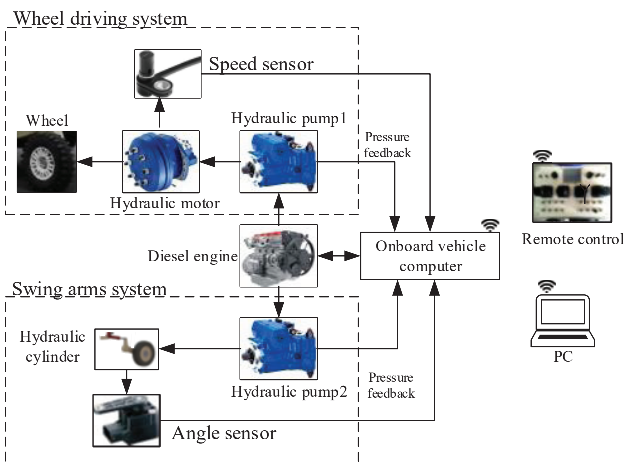

(a) Structure of the platform

(b) Dragon Horse

Fig. 3. the Dragon Horse platform

The remote controller sends the manipulator command to Dragon Horse. Then on-board vehicle computer shifts modes between authentic mode and manual mode following the command, then outputs the control command to a diesel engine, which drives the wheel driving system and swing arms system respectively. And the ground-station computer is used to monitor the running state of Dragon Horse, based on a wireless date transmission module. And all the commands on Dragon Horse are based on the CAN-bus.

III. Obstacle Surmounting Strategy

A. Posture Planning strategy for the swing arms

The swing arms play an important role in surmounting process, can adjust different obstacle heights by planning the posture of the arms. The motion planning process can be represent in Fig. 4.

To determine the optimal posture for the swing arms, an constraint function is build:

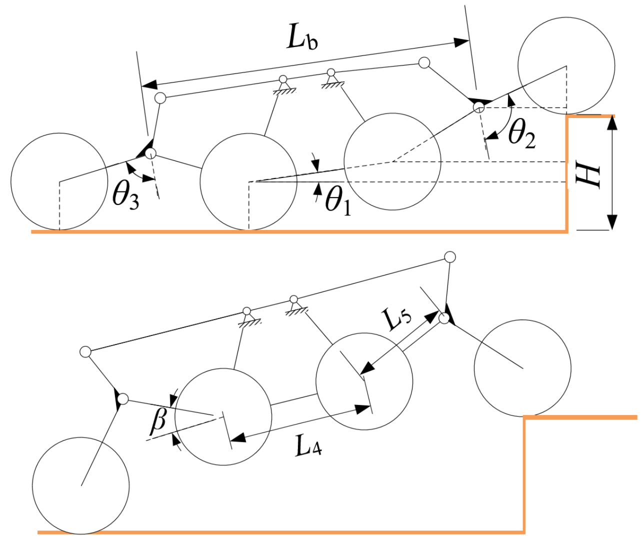

Fig. 4. the Motion Planning Process

$$\begin{aligned} \cos(\theta_2+\theta_1) &= \frac{L_4 \sin\theta_1 + L_5 \sin(\theta_1+\beta) - H}{L_a} \\ \cos(\theta_3-\theta_1) &= \frac{2H-(L_4+L_b)\sin\theta_1 + L_5\sin(\theta_1+\beta)}{L_a} \end{aligned} \tag{9}$$

Based on Eq.9, we can get the relationship between the obstacle height and the radial angles of swing-arms. For the platform has no sensor to detect the height of the obstacle, the θ_2 is set as 110° at the beginning of surmounting process to guarantee the Dragon Horse has the maximum ability to climb the obstacle. While the rear swing arm should follow the constraint function in Eq.9. Dragon Horse needs to drive the arms angle lower than the minimum, $\theta_2 = \theta_3 = 30°$.

B. Gravity Center analysis

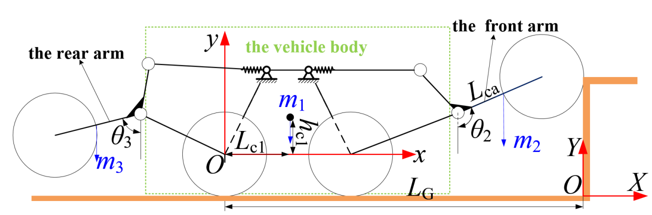

Fig. 5. the Structure of Dragon Horse

The gravity center of UGV is a key factor to determine whether the vehicle can climb an obstacle. Whether the gravity center can climb the obstacle directly means the UGV can do it . It is important to studied the gravity center motion of Dragon Horse. The structure of Dragon Horse can be divided into three parts: the vehicle body, the front arm and the rear arm. As shown in Fig. 5, x-O-y is the body coordinate, and X-O-Y is the world coordinate. The gravity center is at the geometric center. We can obtain the position of each part:

$$\left\{\begin{array}{l} C_1=\left(\frac{L_4}{2}, h_{\mathrm{r}}\right) \\ C_2=\left(L_4+L_5 \cos \beta+\frac{L_a \sin \theta_2}{2}, L_5 \sin \beta-\frac{L_a \cos \theta_2}{2}\right) \\ C_3=\left(-L_5 \cos \beta-\frac{L_a \sin \theta_3}{2}, L_5 \sin \beta-\frac{L_a \cos \theta_3}{2}\right) \end{array}\right. \tag{10}$$

The relationship function in the vehicle coordinate can be expressed as:

$$\left\{\begin{array}{l} x_m=\dfrac{m_1 \dfrac{L_4}{2}+m_2\left(L_5 \sin \beta+L_4+\dfrac{L_a}{2} \mathrm{s}_2\right) +m_3\left(-L_5 \sin \beta-\frac{L_a}{2} \mathrm{s}_3\right)}{m_1+m_2+m_3} \\ y_m=\dfrac{m_1 h_{c1}+m_2\left(L_5 \cos \beta-\dfrac{L_a}{2} \mathrm{c}_2\right) m_3\left(L_5 \cos \beta-\dfrac{L_a}{2} \mathrm{c}_3\right) +m_3\left(L_5 \cos \beta-\frac{L_a}{2} \mathrm{c}_3\right)}{m_1+m_2+m_3} \end{array}\right. \tag{11}$$

In the world coordinate X-O-Y:

$$\left\{\begin{array}{l} X_m=x_m-L_G \\ Y_m=y_m+R \end{array}\right. \tag{12}$$

where h_C1 is the y-$axis$ position in the vehicle body, C_i and m_i are the parts coordinate and mass, L_G is the distance between the origins of two coordinates, and the s_i, c_i are the abbreviations for $sin\theta_i$, $cos\theta_i$.

C. Surmount Obstacle

To guarantee the Dragon has the maximum ability of obstacle surmounting, a dynamic analysis of surmounting an obstacle is performed. Here, there is a assumption that the surmounting process is low speed. And so it is in the real world. Cause the front and middle wheels have a tremendous effect when surmounting an obstacle, they need a instantaneous torque to do it. So, it is reasonable for us only analysis the motion of front and middle wheels.

The quasi-static surmounting model of the front wheels is shown Fig. 6(a). In the surmounting process, the dynamic expression of Dragon Horse can be expressed:

$$\left\{\begin{array}{l} N_1 \varphi+N_{a2}(\varphi \sin \alpha-\cos \alpha)=0 \\ N_1+N_{a2}(\varphi \cos \alpha+\sin \alpha)-G=0 \\ N_1\left(\varphi H-x_1\right)+G x_m=0 \end{array}\right. \tag{13}$$

We can get the expression of the α and θ_1, based on the geometric analysis:

$$\sin \alpha=1+\frac{A-H}{R} \tag{14}$$

where

$$A=L_4 \sin \theta_1+L_5 \sin \left(\theta_1+\beta\right)-L_a \cos \left(\theta_1+\theta_2\right) \tag{15}$$

We can get the constraint function of H:

$$H\left(\theta_1, \varphi\right) \leq H \leq H\left(\theta_1\right) \tag{16}$$

where $H(\theta_1, \psi)$ is the ground attachment function, $H(\theta_1)$ is the planning constraint function, and ψ is the attachment

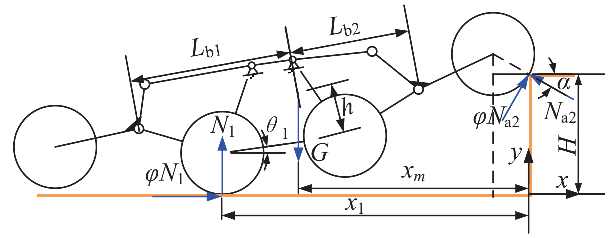

(a) the Front Wheels

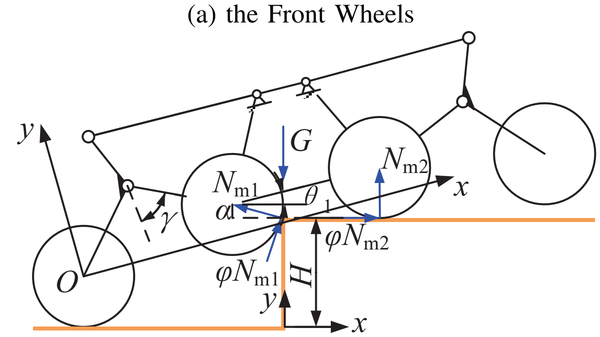

(b) the Middle Wheels

α represents the angle between the normal contact force and horizontal direction, $N_i$represents the ground contact force of each wheel, θ is the adhesion coefficient.

Fig. 6. Surmounting an Obstacle

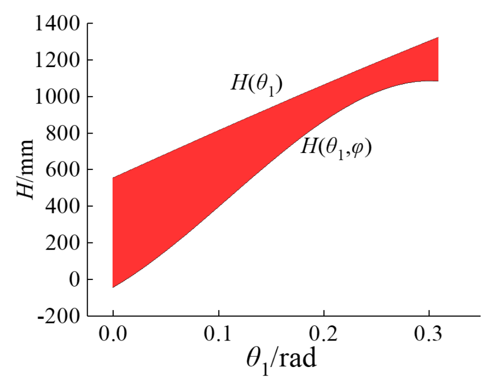

Fig. 7. the Obstacle surmounting ability of the front wheel

coefficient value. Then, we can obtain the front wheels surmounting constraint plot as in Fig. 7.

The middle wheels surmounting process is as show in Fig. 6(b). During the contacting process, the rear wheels are off the road, so the related contact force can be ignored. The dynamic expression of middle wheels can be obtained:

$$\left\{\begin{array}{l} N_{m1}(\varphi \sin \alpha-\cos \alpha)+N_{m2} \varphi=0 \\ N_{m1}(\varphi \cos \alpha+\sin \alpha)+N_{m2}-G=0 \\ N_{m1} \varphi R+N_{m2}\left(L_4 \cos \theta_1+\varphi R \sin \alpha\right) \\ -G R \cos \alpha=0 \end{array}\right. \tag{17}$$

Follow Eq.14, we can get:

$$\sin \alpha=1+\frac{L_a \cos \left(\theta_3-\theta_1\right)-L_5 \cos \left(\gamma+\theta_1\right)-H}{R} \tag{18}$$

Based on the geometric analysis, the obstacle expression can be obtained:

$$H' = R + L_a \cos(\theta_3 - \theta_1) - L_5 \cos(\gamma + \theta_1) \tag{19}$$

To make sure the platform can climb the obstacle, the gravity center of Dragon Horse should be cross over the obstacle edge. The expression in Eq.19 should be rewritten as:

$$\begin{aligned} H =& R + x_m \sin\theta_1 + y_m \cos\theta_1 - 2R\sin\alpha \\ & - \frac{x_m - L_a \sin\theta_3 - L_5 \sin\gamma - R}{\sin\theta_1} \end{aligned} \tag{20}$$

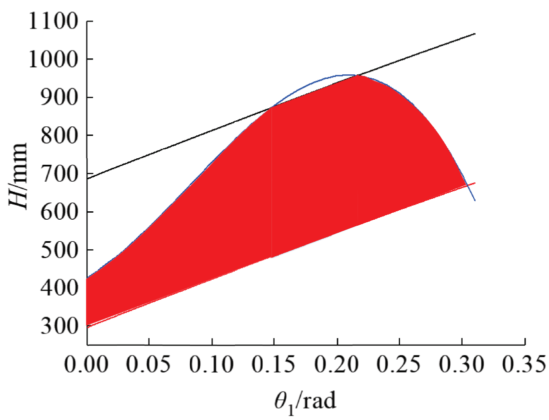

Fig. 8. the Obstacle surmounting ability of the middle wheel

Following the constrain Eq.18-21, then, we can get the obstacle surmounting curve(Fig. 8),and get the maximum height value of the obstacle, which Dragon Horse can surmount: $H = 957mm$.

IV. Surmounting Experiment

A. Platform

To better verify the mechanism kinematic and the surmounting ability of Dragon Horse, a simulation is carried out in the ADAMS and a real Dragon Horse is build as shown in Fig. 3. The parameters of Dragon Horse are show in TABLE. 1.

B. Experiment

The surmounting simulation is shown in Fig. 9, The simulation result show that this kind of UGV can climb an obstacle for 950mm height. and the experiment on the Dragon Horse is conducted as show in Fig. 10.

TABLE I
The Parameters of Dragon Horse

Parameter	Name	Value
m_1	weight(kg)	3,200
T	wheel motor torque(Nm)	4,047
L_4	intermediate wheelbase(mm)	1,000
L_5	bevel chassis length(mm)	1,000
L_b	Dragon Horse length (mm)	2,900
β	chassis approach angle(degree)	18

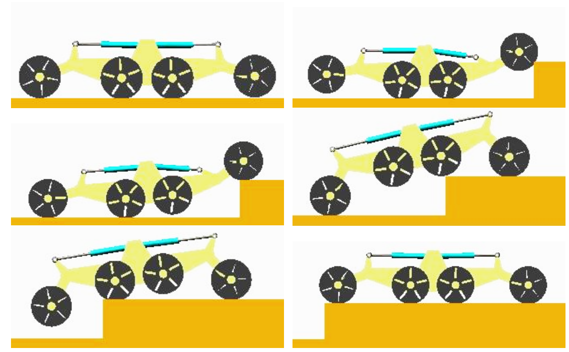

Fig. 9. Simulation

Fig. 10. Experiment

The experiment results show that the Dragon Horse can surmount an 950mm height obstacle. The position track of swing arm wheel is a swing cycle, shown in Fig. 11.

The posture planning results of simulation and experiment are shown in Fig. 12. The curves show that the experiment results are well agree with the simulation ones, verify the planning strategy is efficient. The swing arms angle range is from 30° to 110° Cause the frequent collision between the wheel tires and obstacle surface, the swing angle changes instantaneously with the spring action of the hydraulic cylinder,

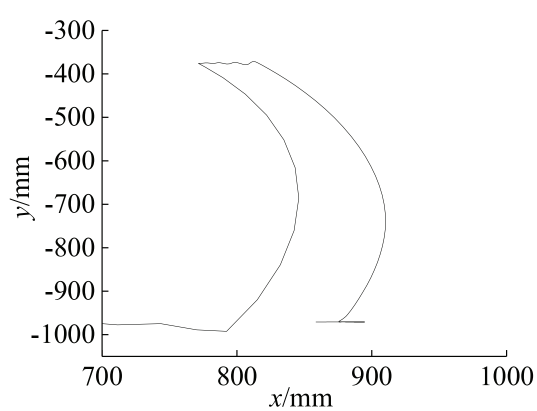

Fig. 11. the Trace of swing arm wheel

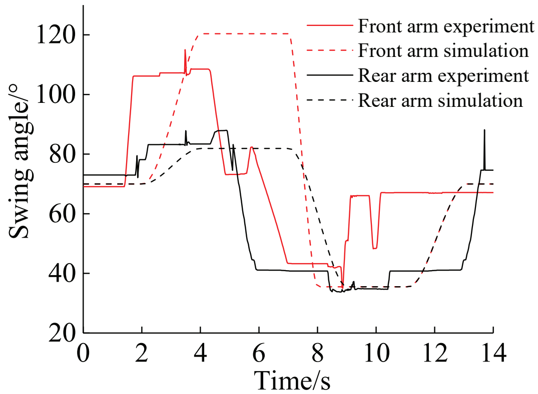

Fig. 12. the Posture planning results of simulations and experiments

and the maximum transient angle is about $10°$. The hydraulic cylinder needs a excellent cushioning performance for field operations.

The wheel tires in simulation model are rigid, while the actual tires will undergo deformation during the obstacle surmounting process, so the ground contact force in simulation is smaller than experiment one. The torque is larger than the rear wheels one during surmounting process. That means the front and middle wheels are very difficult during climbing. Based on the simulation toques requirement for 2657 Nm and the platform payload, choosing a maximum 4047 Nm output for the wheel hydraulic motors is reasonable.

V. Conclusion and Future Work

To meet the adaptation requirement of UGV on unstructured terrain and improve the UGV adaptive ability, we propose a novel horse inspired UGV "Dragon Horse", drived by a distributed hydraulic motors. we study the horse inspired concept and kinematic model to guarantee the platform has sufficient motion ability. Then, we analyze the the dynamic performance of Dragon Horse in detail. Finally, ADAMS simulation and surmounting experiment are conducted to verify the efficiency of this type of vehicle, which can surmount a 950mm height obstacle. In the future, we will focus on improving the environmental perception and high level autonomous ability of Dragon Horse, using Lidia sensors with CKF [17] to realize environmental perception, and cooperating with our aerial robot platform [18] to improve the ability of environmental exploration.

References

[1] He, M., He, J., Zhou, X. Robust flight control of a small unmanned helicopter. Jiqiren/Robot, 2016, pp.337–351.

[2] Bruzzone, L., Quaglia, G. locomotion systems for ground mobile robots in unstructured environments. Mechanical Sciences, 2012,3(2), pp.49-62.

[3] Chen, H. Y., Yu, Z. . An Overview of Research on Military Unmanned Ground Vehicles. Acta Armamentarii, 2014,35(10), pp.1696-1706.

[4] He, Miaolei, Jilin He, and Sebastian Scherer. "Model-based real-time robust controller for a small helicopter." Mechanical Systems and Signal Processing 146: 107022.

[5] M. He and J. He, Extended State Observer-Based Robust Backstepping Sliding Mode Control for a Small-Size Helicopter, IEEE Access, 2018. pp.33480-33488,

[6] Conduraru, A., Doroftei, I., Conduraru, I. . An Overview on the Design of Mobile Robots with Hybrid Locomotion. Advanced Materials Research, 2013, 837(837), pp.555-560.

[7] Suzumura A, Fujimoto Y. Real-time motion generation and control systems for high wheel-legged robot mobility[J]. IEEE Transactions on Industrial Electronics, 2013, 61(7),pp.3648-3659.

[8] Luo Y, Li Q, Liu Z. Design and optimization of wheel-legged robot: Rolling-Wolf[J]. Chinese journal of mechanical engineering, 2014, 27(6): pp.1133-1142.

[9] Luo R C, Hsiao M, Lin T W. Erect wheel-legged stair climbing robot for indoor service applications[C]//2013 IEEE/RSJ International Conference on Intelligent Robots and Systems. IEEE, 2013: 2731-2736.

[10] Bai L, Guan J, Chen X, et al. An optional passive/active transformable wheel-legged mobility concept for search and rescue robots[J]. Robotics and Autonomous Systems, 2018, 107, pp.145-155.

[11] Kim, Y. S., Jung, G. P., Kim, H., Cho, K. J., Chu, C. N. Wheel Transformer: A Wheel-Leg Hybrid Robot With Passive Transformable Wheels. IEEE Transactions on Robotics, 2014, 30(6), pp.1487-1498.

[12] Sun, T., Xiang, X., Su, W., Wu, H., Song, Y. A transformable wheel-legged mobile robot: Design, analysis and experiment. Robotics and Autonomous Systems, 2017, 98, pp.30-41.

[13] Siegwart, R., Lamon, P., Estier, T., Lauria, M., Piguet, R. Innovative design for wheeled locomotion in rough terrain. Robotics and Autonomous Systems, 2002, 40(2), pp.151-162.

[14] Grand, C., Benamar, F., Plumet, F., Bidaud, P. Stability and Traction Optimization of a Reconfigurable Wheel-Legged Robot. The International Journal of Robotics Research, 2004, 23(10-11), pp.1041-1058.

[15] Gray, J.P., Vantsevich, V.V., Overholt, J.L., Indices and Computational Strategy for Unmanned Ground Wheeled Vehicle Mobility Estimation and Enhancement. Proceedings of ASME 2013 IDETC, Paper No. DETC2013-12158, USA; 2013.

[16] Valois, J.S., Herman, H., Bares, J. and Rice, D.P., Remote operation of the black knight unmanned ground combat vehicle, Proceedings of SPIE The International Society for Optical Engineering, 2008, 6962, pp. 69621A-1-69621A-11.

[17] He, Miaolei, and Jilin He. "A Dynamic Enhanced Robust Cubature Kalman Filter for the State Estimation of an Unmanned Autonomous Helicopter." IEEE Access 7 (2019): 148531-148540.

[18] M. He and J. He, Modeling and robust attitude controller design for a small size helicopter, in Proc. IEEE Int. Conf. Ind. Technol. (ICIT), Feb. 2019, pp. 145150.